IEEE Access
Multidisciplinary | Rapid Review | Open Access Journal

Received May 16, 2021, accepted May 27, 2021, date of publication June 10, 2021, date of current version June 28, 2021.

Digital Object Identifier 10.1109/ACCESS.2021.3088236

Wood Product Tracking Using an Improved AKAZE Method in Wood Traceability System

YONGKE SUN[1], GUANBEN DU[1], YONG CAO[2], QIZHAO LIN[2], LIHUI ZHONG[3], AND JIAN QIU[3]

[1]Yunnan Provincial Key Laboratory of Wood Adhesives and Glued Products, Southwest Forestry University, Kunming 650224, China
[2]College of Big Data and Intelligence Engineering, Southwest Forestry University, Kunming 650224, China
[3]College of Material Science and Engineering, Southwest Forestry University, Kunming 650224, China

Corresponding authors: Yong Cao (cn_caoyong@126.com), Guanben Du (gongben9@hotmail.com), and Jian Qiu (qiujian@swfu.edu.cn)

This work was supported in part by the Program for Leading Talents of Science and Technology in Yunnan Province under Grant 2017HA013, in part by the National Natural Science Foundation of China under Grant 61462095, in part by the Major Project of Science and Technology of Yunnan Province under Grant 202002AD080002 and Grant 2019ZE005, and in part by the Joint Agricultural Project of Yunnan Provincial Department of Science and Technology under Grant 2018FG001-108.

ABSTRACT Tracking of the wood product is an important technology in the trade activity of rare plants. Normally, the factories use Quick Response (QR) and Radio-Frequency Identification (RFID) to identify the individual wood product, but these technologies are not safe enough because they can be easily falsified. It can be seen that traditional methods are hard to catch the detail of the slim wood texture from the wood product. In this study, a novel method is employed to resolve these problems using a biometric feature on the surface of the real wood product to distinguish the individual wood product. AKAZE is used to extract the key-point of wood texture. A sub-area detection technique along with a serialization method is then developed to improve the rate of identification. The sub-area detection technique deals with picking out a sub-region in which there are enough AKAZE points as small as possible. The serialization method is also utilized to reduce the redundant process of feature extraction. The experimental results demonstrate that the values of accuracy, recall, and $F1$ reach 0.98, 0.96, and 0.96, respectively. The match time that uses serialized function is reduced to 1/3 of which has no application in the original image. The validated results also reveal that our proposed methodology improves the robustness of the wood product identification, and it can be used in Wood Traceability System (WTS) with the blockchain to resolve the digital trust problem and the fast distinction issues of the real wood product.

INDEX TERMS Wood identification, AKAZE, trust label, blockchain.

I. INTRODUCTION

Wood is an important natural resource and due to the high demand for wood products, most rare plants suffer from illegal logging. The endangered plants in Convention on International Trade in Endangered Species (CITES) list [1] have been prohibited from trading, which has led to the high price of the rare woods. Forgers make wood products with low price woods to falsify the rare products and sell at a high price. The wood product identification is a necessary method to certify whether the product is genuine or fake [2].

Wood Traceability System (WTS) is a technology used to trace the product information. In relevant factories, the information related to wood products is written and saved in the traceability system. Quick Response (QR) and Radio-Frequency Identification (RFID) are employed as labels stuck in the wood surface to identify the individual wood product. The customer gets the required information which includes the wood species by scanning the label [3], [4], and does not send it to the lab for identification. It is convenient for customers to get the results quickly. However, this kind of label is easy to be falsified [3] by copying or transforming onto the other, and it is not safe and secure at all.

Deoxyribonucleic Acid (DNA) is a technology used to identify the wood species and prevent falsifying of the wood product [5]–[8], and it is a high-accuracy technology than the others. However, acquiring the DNA sequence is costly and time-consuming, and it is not suitable for the wood product because it is hard to extract the DNA from the dried wood [9].

The associate editor coordinating the review of this manuscript and approving it for publication was Yizhang Jiang.

Furthermore, the DNA technology cannot distinguish the individual wood product made from the same tree.

On the other hand, image recognition technology is a fast and cost-effective method that can be also employed to identify the wood product. Taking the wood image using a microscope or magnifying glass, and classifying the wood species with computing models such as neural networks or deep learning models are the two most discussed topics in this field. In recent years, the methods based on the image have succeeded in wood species recognition [10]–[14]. R.Schraml and H.Hofbauer attempted to use the fingerprint and iris recognition methods to distinguish the individual wood entities [15]. According to the performed experiments, they used cross-sectional images of the log distinguished individual wood entities with high accuracy around 93%. The findings revealed that the wood texture is unique, and it is feasible to identify the individual wood product using the wood texture.

Detecting and describing key-points are important functions in the identification of images. The key-points are those which have significantly different gray values from their neighbors [16], [17]. Scale-Invariant Feature Transform (SIFT) [18], Speeded Up Robust Features (SURF), and Oriented FAST and rotated BRIEF (ORB) [19] are among the three main image key-point extraction methods. SIFT has good interference ability for noise, rotation and zoom [20], [21], and it is often utilized to recognize the face [22], animal [23], and object [24], [25]. SURF is a variant of SIFT that has good performance of affine-transformation invariant and fast speed [26], even can be used to trace objects in real time [27]. ORB is another invariant and resistant-to-noise method, which has the fastest speed of descriptor extraction [28]. However, all these approaches are based on the Gaussian blur methods that smooth the noise in the image. In fact, most of the wood product surfaces have rich slim textures that are difficultly detected by SIFT, SURF, and ORB methods.

AKAZE is a nonlinear diffusion filtering method that focuses on the texture, and not the color patches [21], [29], which can detect the features of the slim textures. Furthermore, since the wood structure is anisotropy [30], it is regarded as the uniqueness of the wood product. Therefore, it can be also utilized to distinguish the individual wood product. In this study, we propose a novel method based on the AKAZE algorithm to identify individual wood products. A sub-area detection method and a serialization method are also employed to improve the matching speed. The sub-area detection method is to find a sub-region of the image which has enough key-points, and the serialized method is to store and restore the key-points from the structured data.

Blockchain is a method to resolve the security problem of the digital data [31], [32]. It succeeded in the Bitcoin system in 2009, and was rapidly used in the agricultural supply chain due to the security and the transparency [33]. The wood blockchain that we are researching is similar to the agricultural blockchain, and it is a data-trusted technology that can be used to store the digital information about the wood products in the WTS [34]. It offers trusty information for both protection organizations and consumers, and also offers the identification and relevant information about the wood product. Furthermore, it can increase the acceptance of the customers [35], [36].

The workflow of our designed WTS is shown in Fig.1. Two processes are involved in this system. The first process is related to uploading, which includes acquiring the wood product image and then using a key-point detection method to extract the feature and crop a sub-region as the criterion image. The second process is the identification, in which the characterized feats in the traceability system and the customer image are compared by calculating the similarity between them.

In the upload process, three steps are executed sequentially (see Fig.2). The first step seeks all key-points of the images, the second step tries to pick a sub-region of the image as a criterion image, and the third step serializes the features of the sub-region into structured text data. The matching operation compares the customer image and the serialized features stored in the traceability system. In the traditional method, the criterion images are stored in the traceability system. It needs a key-point detection and descriptor calculation during the matching process. In our proposed method, we store the serialized feature instead of the image in the traceability system, these features can be read directly, and the processing of the key-points finding as well as descriptor calculation is no longer needed. The improved process is represented by Fig.3. Firstly, the AKAZE key-points are detected. Secondly, the descriptors of them are calculated. Finally, all key-points from the customer image and key-points are matched which are un-serialized from the criterion image serialized data stored in the traceability system.

The number of matched key-points is similar between the criterion image and customer image. If the matched number is larger than the threshold, the wood product is considered as the one registered in the traceability system.

II. PROBLEM FORMULA

Our proposed method contains two important processes named serialized process and identification process. Define $I_m \in R^2$ as an image, and the serialized process is represented by formula (1).

$$string = f_3(f_2(f_1(I_m))) \tag{1}$$

where the transform f_1 is AKAZE method, it extracts all AKAZE points from the image I_m, the f_2 is a key-point filter function that picks a subset of the AKAZE points, and f_3 is a serialization function that packs the picked key-points into a data structure as the identifier of the wood product.

When identifying the wood product, the image I'_m that is obtained from a different camera is compared to the serialized data. The identification process works as follows. First, it calculates the AKAZE key-points of the image I'_m, which is

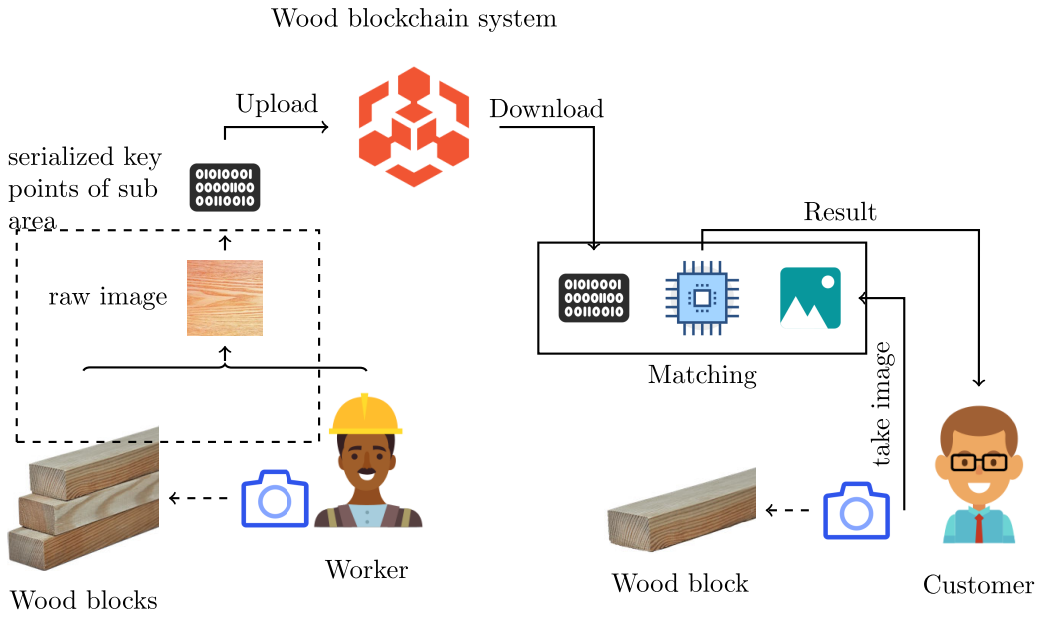

FIGURE 1. Workflow of Individual wood identification. We decreased the data size in the dashed box and improved the computing efficiency in the matching process.

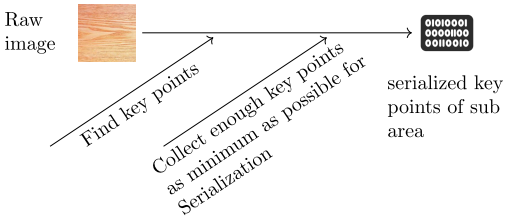

FIGURE 2. Improved upload process. A feature data set of key points was chosen and uploaded to the blockchain system.

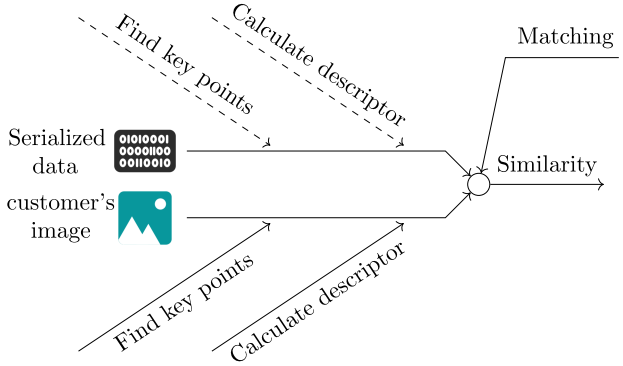

FIGURE 3. Matching process. Our method removes the traditional processes drew with dashed lines and increases the matching efficiency.

represented by formula (2).

$$K_1' = f_1(I_m') \tag{2}$$

Second, it restores the picked key-points from the serialized data using formula (3).

$$k_2 = f_3^{-1}(string) \tag{3}$$

Third, it matches the points set K_1' and the K_2 using KNN function m_{knn}, and gets a matched data set M_{knn}.

$$M_{knn} = m_{knn}(K_1', K_2) \tag{4}$$

Fourth, it rechecks the matched pairs and picks out the best-matched pairs using formula (5).

$$M_{opt} = O(M_{knn}) \tag{5}$$

Finally, it counts the number of the best-matched pairs using formula (6). If the number c is larger than a threshold, it means that the image I_m' and serialized feature *string* come from the same wood product(7).

$$c = count(M_{opt}) \tag{6}$$

$$Identification = \begin{cases} 1 & c \geq threshold \\ 0 & c < threshold \end{cases} \tag{7}$$

III. METHODS

Here, the AKAZE method is proposed to detect the key-points of the image. The AKAZE method is a nonlinear diffusion algorithm that focuses on the edges and keeps the wood rays better than the Gaussian blur method. It employs the heat conduction equation defined as formula (8) to process the image.

$$\frac{\partial L}{\partial t} = div(c(x, y, t) \cdot \nabla L) \tag{8}$$

where *div* is the respective divergence and ∇ stands for the gradient operators. Conductivity function c is defined by formula (9).

$$c(x, y, t) = g(|\nabla L_\sigma(x, y, t)|) \tag{9}$$

where ∇L_σ is a Gaussian smooth function, and the function g contains two different types which are given by formula (10) (11).

$$g_1 = exp(-\frac{|\nabla L_\sigma|^2}{k^2}) \tag{10}$$

$$g_2 = \frac{1}{1+\frac{|\nabla L_\sigma|^2}{k^2}} \tag{11}$$

where k is the contrast and the g_2 is the default diffusion function used in the library of the OpenCV.

1) KEY POINT

AKAZE picks up the key-points using an O octaves and S sub-levels pyramid. The corresponding scale σ is shown by formula (12).

$$\sigma_i(o,s)=2^{o+s/S},\ o\in[0,\ldots,O-1],\ s\in[0,\ldots,S-1] \tag{12}$$

where i is the image index in the pyramid. For the purpose to simulate the conduction equation, AKAZE maps the σ to the t which is displayed by formula (13).

$$t_i = \frac{1}{2}\sigma_i^2 \tag{13}$$

Assume the image is L, then the filtered image in the pyramid is calculated by formula (14).

$$L^{i+1} = (I - (t_{i+1} - t_i)\sum_{l=1}^{m} A_l(L^i))^{-1}L^i \tag{14}$$

where $A_l(L^i)$ stands for the conductivity matrix of the L^i,

A Hessian matrix is then used to detect the interest points. The image of different sizes needs to be normalized with respect to scale [37] with formula (15). After finding the Hessian matrix, the points with higher gray values than neighbors are picked up as the key-points. Normally, the neighbors are narrowed in a 3 × 3 size [38].

$$L_{Hessian} = \sigma^2(L_{xx}L_{yy} - L_{xy}^2) \tag{15}$$

2) DESCRIPTOR

The proposed AKAZE utilizes an invariant-rotation descriptor to increase the matching robustness. The first step is finding the dominant orientation by defining a circle whose center is the key-point and its radius is $6\sigma_i$, and then is divided into 6 parts with $\pi/3$ degrees. The domination orientation is the same as the orientation of which the sliding segment has the longest derivative responses [39], [40]. The derivative of the segments is the sum of the L_x and the L_y. In Fig.4, the right-upper segment represents the dominant orientation because it has the longest derivative. The dominant orientation is the direction of the first segment, and the angle is θ.

Actually, AKAZE uses the M-SURF descriptor that is employed in the SURF method to describe the key-points. A 24 × 24 square whose center is the key-point is rotated to the dominant orientation with angle θ which is applied to calculate the features with neighbor pixels [37].

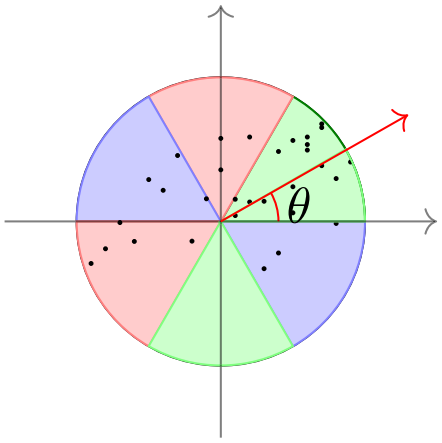

FIGURE 4. Orientation. The first sliding segment represents the orientation because it has the longest derivative responses.

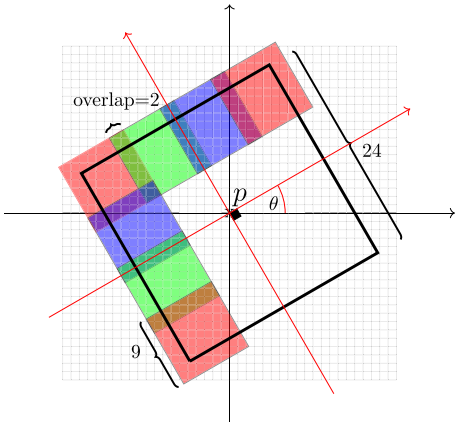

FIGURE 5. Descriptor. Every sub-region uses 4 decimals to present and the square has 16 sub-regions, so, each key point has 64 decimal data.

Fig.5 illustrates this process, first, divides the square into 4 × 4 sub-regions with 2 overlaps, and then calculates the features d_v for every sub-region. The feature d_v is represented by formula (16). Since each sub-region has 4 features, a vector of one key-point includes 64 feature data.

$$d_v = (\sum L_x, \sum L_y, \sum |L_x|, \sum |L_y|) \tag{16}$$

where, L_x and L_y are the first-order derivatives of the sub-region over different octaves.

A. SUB IMAGE

Since extraction of the key-points from a small sub-area is faster than the original image, we design a new distance-based technique to pick up the sub-area as minimum as possible, which contains at least 500 key-points. Here, the threshold of 500 came from the statistics of the relevant experiments. The workflow of the criterion image selection is shown in Fig.6, in which it collects all key-points of the whole image. It calculates the center of the image and marks (x_c, y_c), defines an initial distance threshold $r = 48$, measures all the distances between the center point and every key-point, and finally, collects those with distances shorter than the

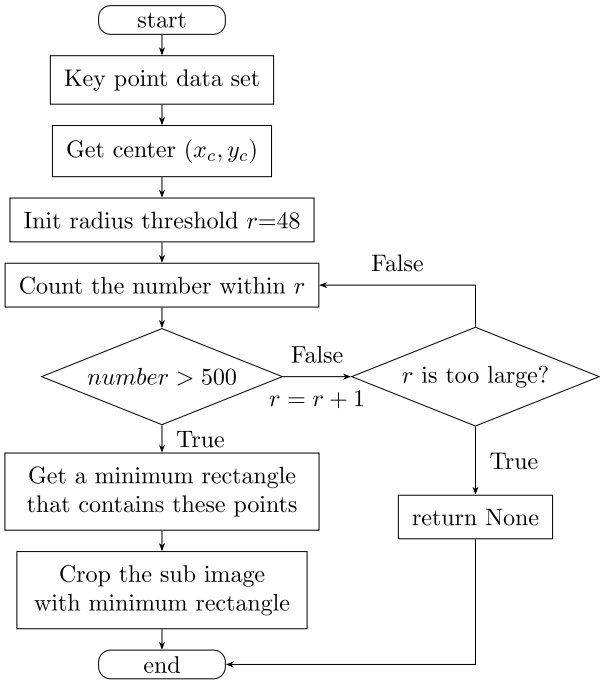

FIGURE 6. Workflow of the processing of the sub-image extraction.

threshold r. If the collected size is less than 500, the distance threshold r is increased and it recollects again. The loop escapes when enough key-points are collected or the threshold r is larger than the image size.

If there are enough key-points collected, a minimum rectangle that contains enough key-points will be then picked up. This sub rectangle is the criterion image. If the threshold r is out of the image and still has no enough key-points collected, the process will return none, which means that this image is not suitable for this method.

The algorithm 1 illustrates the process of the criterion image calculation. A raw image and key-point list are needed. The program calculates the distance between the center point and every key-point. In order to collect enough key-points, the variable r is limited between 48 pixels and the maximum width and height of the image.

Algorithm 1 Getting the Sub-Image and the Key Points

Require: Image and key point list
Ensure: sub-image and key points

```
Define a minimum radius, r=48 pixels
center=image center
Rect=[]
for r=48 to max(image.width/2, image.height/2) do
    selected_keys=[]
    for l=0 to length(keyPoints) do
        d= distance(center,keyPoints[l])
        if _d <= r then
            selected_keys.push(keyPoints[l])
        end if
    end for
    if len(selected_keys)>=500 then
        Rect=Rectangle(selected_keys)
        break
    else
        r = r + 12 /*increasing the pre-distance*/
    end if
end for
if Rect==[] then
    return None
else
    return image[Rect],selected_keys
end if
```

B. SERIALIZING

The selected key-points are defined by SK, the serialized key-points $sk, sk \in SK$ are given by formula (17). Finally, sk_i has 2 data expressing the key-point position and 64 data expressing the descriptor. The total length is 66 data.

$$sk_i = [x, y, d_{v1}, d_{v2}, \ldots, d_{v64}] \tag{17}$$

The serialized feature of the sub-region is a vector given by formula (18).

$$img = [sk_1, sk_2, \ldots..sk_k], k \approx 500. \tag{18}$$

C. MATCHING

The similarity is determined by the number of matched points. The k-NN algorithm [41], [42] is employed to calculate the nearest neighbors. According to the principle of the k-NN algorithm, every key-point has k matched points, but some matched points are not similar. For this purpose, filtering the good matched points, the parameter $k = 2$ is adopted to get two Nearest key-points [43]. A key-point in the first image is defined as K_{Ao}, and the first two nearest key-points in the other image are K_{Bm} and K_{Bn}. The Hamming distance [44] from K_{Ao} to K_{Bm} is d_1, and the distance from K_{Ao} to K_{Bn} is d_2. Only the distance $d_1 \leq d_2 \times 0.6$ the points K_{Ao} and K_{Bm} is considered to be a good match.

The key-points come from the same position on the wood surface to meet a project function. Random Sample Consensus (RANSAC) is an iterative method to estimate the project parameter [45]. In experiments, it is usually used to remove the outlier key-points once again and keep those that adhere to the RANSAC project function. A threshold N used to judge two images are defined to be from the same wood product image. The minimum of the N is 4 because the RANSAC needs more than four matched points to estimate the project function.

D. SIMILARITY

The similarity of the image a with serialized data set C is defined by sim. The $matche\_points(a, c_j), c_j \in C$ is the number of matched points of image a and serialized feature c_j. $sim(a, c_j)$ is defined by formula (19). It means that a is compared with $c_j \in C$ and returns the one with the largest

FIGURE 7. Furniture. The furniture used in our experiments.

FIGURE 8. Wood surface images. Each row came from same furniture surface.

matched point.

$$sim(a, c_j) = max\{matched\_points(a, c_1), matched\_points(a, c_2), \ldots, matched\_points(a, c_n)\} \quad (19)$$

IV. EXPERIMENTS

A. MATERIALS

The images are acquired from precious wooden furniture in the HaoDu furniture company which produces real wood furniture and is located in Yunnan Province, China. As Fig.7 shows, this furniture is a kind of Chinese-style furniture which is valuable and often counterfeited with cheap materials. All images are acquired by three workers using different mobile cellphone cameras and three model cellphones used in the experiment are Huawei Nova7, Huawei Honor 20, and OnePlus 5T.

The same area is taken into account in different positions and by different cameras to acquire more images, where the distance is approximately 40 cm and the angle from the vertical orientation less than 45 degrees. The original image is represented by Fig.8, and the size is approximately 4608×3456 pixels which depends on the cellphone setting. Totally, 720 images are collected.

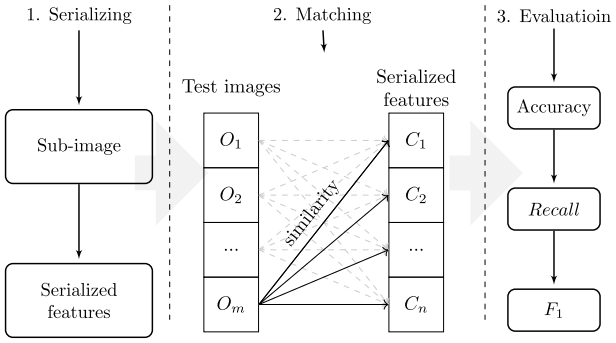

FIGURE 9. Experimental design.

B. EXPERIMENT DESIGN

We simulate the serializing and matching processes and evaluate the identification performance using accuracy, recall, and $F1$, where this experimental workflow is given in Fig.9.

1) EXTRACTING THE FEATURES

In the serializing process used within the uploading sense, a raw image is detected to extract the key-points and serialize the key-points into structured data. In the experiments, the key-point is serialized using formula (17). where (x, y) is the position of the key-point, and d_{vi} represents the descriptor of the key-point. The serialized feature contains 66 digital data.

2) TESTING METHOD

At the matching process, we compare the image with the serialized features stored in the traceability system and calculate the matched points of them. As Fig.9 show, O is defined as the image data set, and the serialized feature is defined as C that is stored in the system. The matched result of the image o_i, $o_i \in O$ is $R(o_i)$ that is calculated by formula (20).

$$R(o_i) = \begin{cases} c_j, & sim(o_i, c_j) \geq N \\ 0, & other \end{cases} \quad (20)$$

where N stands for a threshold of confidence.

3) EVALUATION

In this sub-section, all original images are tested with different thresholds of N. Three evaluation indexes are employed to assert the performance: accuracy, recall, and $F1$ score. The accuracy is a measurement that describes the ability of correct recognition ability, which is calculated using formula (21).

$$accuracy = \frac{TP + TN}{TP + TN + FN + FP} \quad (21)$$

where TP represents the number of true positive detection, FP is the number of false-positive detection, FN shows the number of false-negative detection, and FP is the number of false positive detection.

Precision represented in formula (22) is the proportion of predicted positives that are correct [46], it focuses on the

TABLE 1. Statistical of the correct-matched number with threshold $N = 4$.

Methods	max	mean	std	Z-Score
AKAZE	1783	131.0	167.0	5.08e-17
ORB	1865	27.0	59.0	-3.46e-17
SIFT	1198	30.0	43.0	-2.67e-17
SURF	514	25.0	32.0	-1.02e-17

closeness of the positive recognition, and the high precision means the recognition results are more stable.

$$precision = \frac{TP}{TP + FP} \tag{22}$$

The recall is a proportion of real positive samples that are correctly predicted positive [47] and defined by formula (23).

$$recall = \frac{TP}{TP + FN} \tag{23}$$

Here, $F1$ is a harmonic mean of precision and recall defined by formula(24), that is widely used in uneven class distribution [48].

$$F1 = \frac{2 \times precision \times recall}{precision + recall} \tag{24}$$

where precision and recall calculate using formula (22) and (23)

We also compare the AKAZE with SIFT, SURF, and ORB [28] features extraction methods in the experiments. These methods are used instead of the AKAZE method to calculate the evaluation indexes again. One necessary change is distance measure, the SIFT method employs Euclidean distance [49] to find the neighbors, and the other methods employ Hamming distance [50] to find the neighbors.

V. RESULTS AND DISCUSSIONS

A. MATCHED POINT EVALUATION

The AKAZE method has the best comprehensive performance for the matching because it has the highest Z-Score. A Z-Score is a statistical measurement that describes a score's relationship to the mean of a group of scores, which is presented by formula (25).

$$z = \frac{X - \bar{X}}{\delta} \tag{25}$$

where $\bar{X}$ is the mean of the X, and δ stands for the standard deviation of the X.

A positive Z-Score indicates that the matched points are above the mean, and a negative Z-Score represents the matched points that are below the mean. A higher Z-Score means a better-matched result. Our experiment results are shown in Table 1 and clearly demonstrate that the AKAZE method is the best one because of the highest Z-Score.

The mean of matched points obtained by the AKAZE method is significantly higher than the others, and the reason

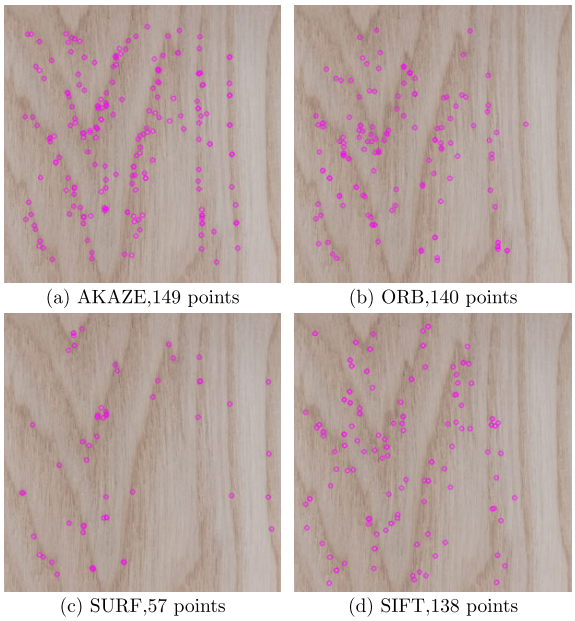

FIGURE 10. Key-points of the wood surface. (*a*) 149 points were detected by the AKAZE method,(*b*) 140 points were detected by the ORB method,(*c*) 57 points were detected by the SURF method, and (*d*) 138 points were detected by SIFT method.

probably is that AKAZE uses a nonlinear diffusion method to blur the image while the other methods employ the Gaussian mean method to do that. Fig.11 displays the contrast between the nonlinear diffusion and the Gaussian, in which the wood rays turn into fuzzy when the Gaussian blur method is applied, but it remains clear when the nonlinear diffusion method is implemented. This comparison reveals that the nonlinear diffusion method is more suitable for the wood texture image.

Fig.10 illustrates a key-point distribution of different methods, in which the key-points are mainly located in the wood rays. The thin texture ignored in the Gaussian method is detected in the AKAZE method. The AKAZE method discovers the most key-points and particularly the key-points located in the wood rays. Moreover, the ORB method detects 140 key-points, but the key-points scatter near the right vertical wood ray. On the other hand, the SURF method only discovers 57 key-points and most of them are located in the wood ray. Finally, the SIFT method detects 138 key-points, but these key-points do not align the wood rays more dispersed than the other methods.

B. THRESHOLD

The $F1$ score is a harmonic measure of the classification system. The higher $F1$ expresses a better recognition performance. We test all images and analyze the recognition results, and the $F1$ score of the different feature extraction methods is shown in Table.2 where the N is the confidence threshold. A significant tendency is that the $F1$ rises with the increase of the N, and the AKAZE method has always the highest $F1$ score.

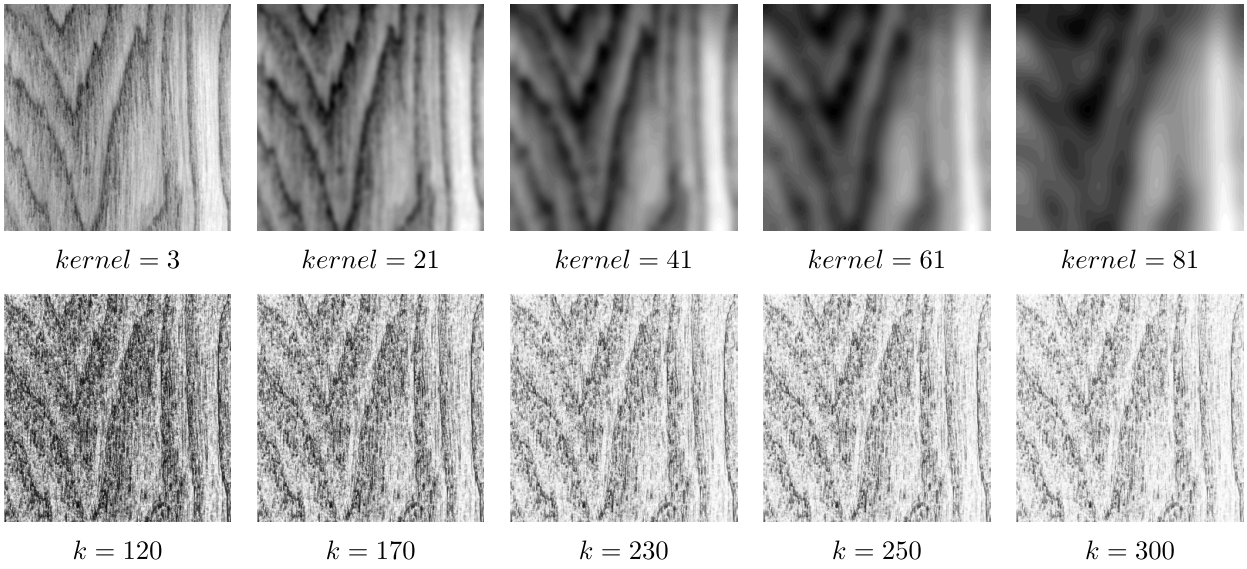

FIGURE 11. A comparison between the Gaussian blur and AKAZE conduction. First row: blurred images with different Gaussian kernel sizes and the *kernel* is the patch size used in the Gaussian. Second row: Nonlinear diffusion scale space and the k is a parameter of the conductivity function g_2.

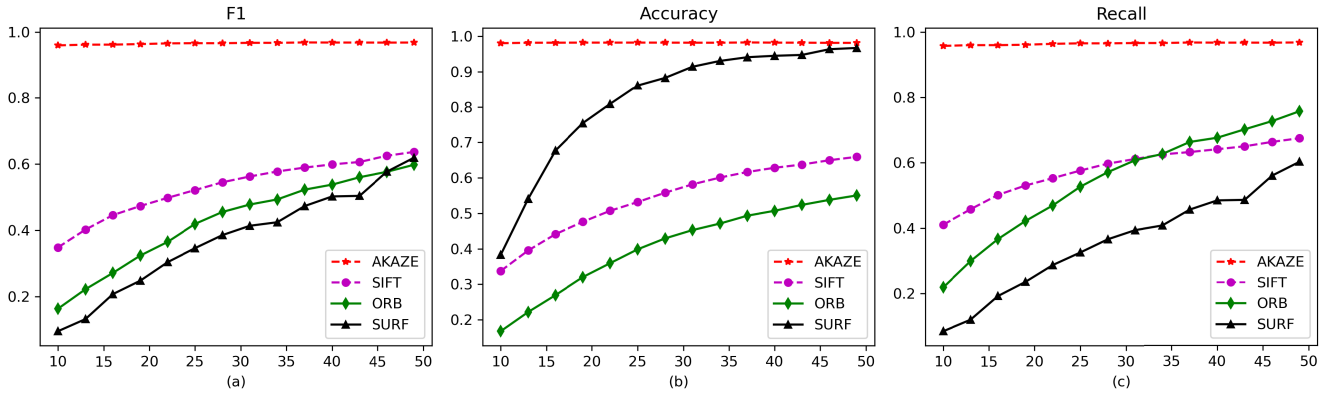

FIGURE 12. A comparison of matching-time with the different methods. The x-axis is the threshold of N.

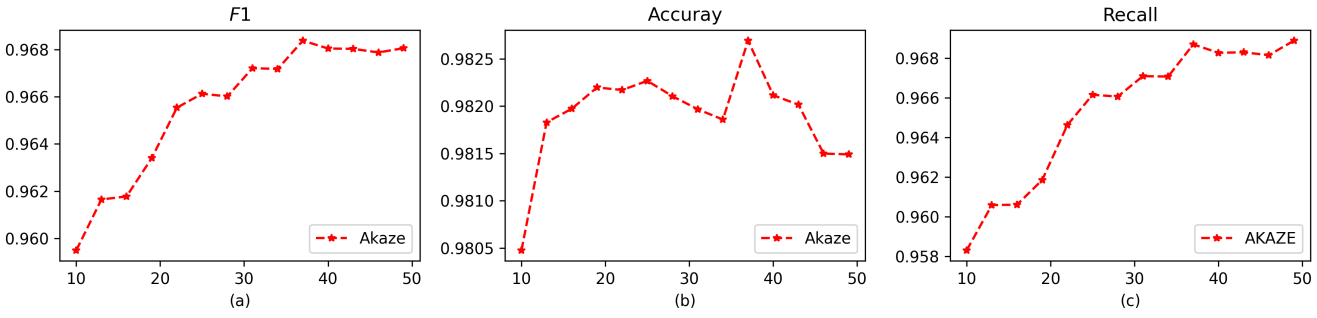

FIGURE 13. $F1$, accuracy and recall under different thresholds N. The maximum of $F1$ sets N=37.

These data also represent that the threshold has less affection for the AKAZE method. With the increasing of the N, the SIFT $F1$, the SURF $F1$, and the ORB $F1$ increase up to 0.289, 0.525, and 0.435, respectively. However, the AKAZE $F1$ increases only up to 0.0086. These data imply that the key-points detected by the AKAZE method are more stable. Due to the images acquired by different devices at different positions, the high recognition rate also means that the

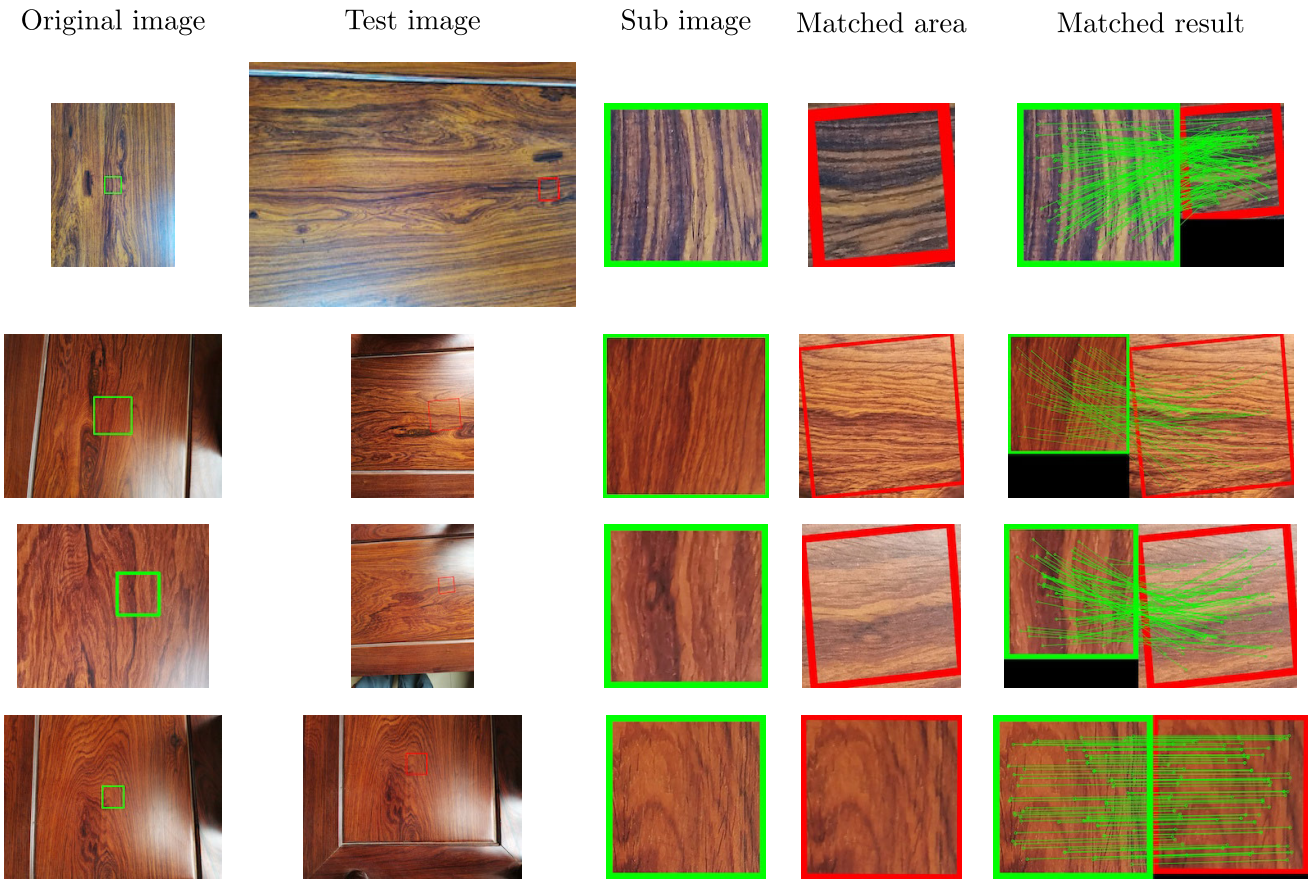

FIGURE 14. Recognition results. Each row comes from different furniture. The first and second columns are captured from the same furniture at different positions, respectively, and the third and fourth columns are zoomed on the first and second columns, respectively. The last column is the matched result, and the threshold $N = 37$.

TABLE 2. $F1$-Score of different methods under different thresholds.

N	AKAZE	SIFT	SURF	ORB
10	0.9595	0.348	0.095	0.163
13	0.9616	0.402	0.132	0.222
16	0.0.9618	0.446	0.207	0.271
19	0.9634	0.474	0.248	0.324
22	0.9655	0.498	0.304	0.365
25	0.9661	0.521	0.346	0.419
28	0.966	0.545	0.386	0.455
31	0.9672	0.563	0.414	0.478
34	0.9672	0.578	0.424	0.493
37	0.9684	0.59	0.473	0.523
40	0.968	0.599	0.502	0.538
43	0.968	0.606	0.504	0.56
46	0.9679	0.625	0.577	0.577
49	0.9681	0.637	0.62	0.598

AKAZE based method has better rotational invariance and blur invariance.

Fig.12 shows the $F1$, accuracy and the recall. We test these three criterion indexes with different methods and thresholds. The obtained results demonstrate that the AKAZE based method has the best performance. The SIFT, ORB, and SURF based methods have different performances in terms of accuracy and recall. For example, the SURF has high accuracy when using threshold $N \geq 40$, while it has the lowest recall.

Although the changing of the AKAZE based method is small, it still has a tendency. The accuracy increases first, and then decreases according to Fig.13, and finally, the recall rate increases. The threshold $N = 37$ is an optimal value of the identification system. When this threshold $N = 37$ is considered, the $F1$ score, accuracy, and recall take the highest value.

Fig.14 displays the matched result when using the threshold =37. The first column is the original image, and the green sub-area is the criterion area that is zoomed in and shown in the third column. The second column is the test image, and the red sub-area is zoomed in from the fourth column. The test images in the second column are acquired from the same furniture at different positions. The last column is the matched result, which states that the method based on the AKAZE algorithm has rotation invariance and robustness.

C. IDENTIFICATION ABILITY

One AKAZE descriptor is a 64-dimensional vector, and each dimension has 8 *bits*. The total length of one descriptor is 64×8 *bits* $= 512$ *bits*, of which combination is 2^{512}. In our experiment, the confidence threshold $N = 37$ means that there are 37 key-points as small as possible demonstrating

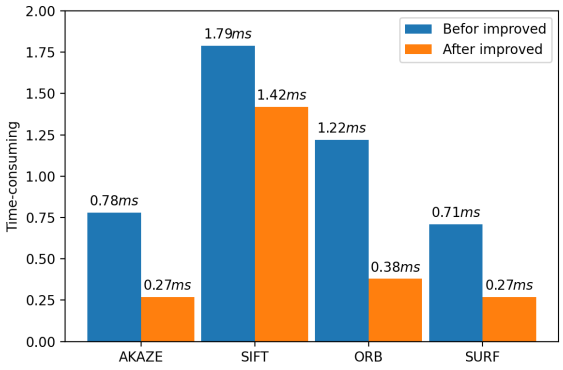

FIGURE 15. Comparison of the matching time between the non-serialized and the serialized method. The y-axis is the mean of the matching time per image.

the correct identification. The identification space is given by formula(26).

$$(2^{512})^{N=37} \tag{26}$$

AKAZE uses Hamming distance to measure the similarity. According to the statistics of the correct matched points, the mean distance is 50, and the standard deviation is 20. The small distance implies that the AKAZE based method has better identification space, and the big distance indicates that the AKAZE based method has a small identification space. The minimum identification space Ω_{min} is calculated using a big distance 70, which is represented by formula(27).

$$\Omega_{min} = (2^{512-70})^{37} \tag{27}$$

The identification space is a theoretical basis for wood product identification in traceability. In theory, the Ω_{min} is a huge number, and it reveals that this method has enough ability to identify every woodblock.

D. IDENTIFICATION SPEED

The advantage of the traceability system is data security, but the transmission speed is a bottleneck. The serializing process reduces the data size significantly. For example, raw image size is usually 4608 × 3456 pixels, and the serialized feature approximate has 500 × 66 data. The data size shrinks to 0.002 times the raw image. The small data size means less time is needed to transmit the data.

Fig. 15 displays the difference of the matching time between the non-serialized and serialized methods, and clearly shows that the comparison time is reduced by the serialized method. The comparison time of matching for once is approximately deduced to 1/3 in the AKAZE method. For SIFT, ORB, and the SURF methods, the serialized method also reduces the matching time significantly.

The serialized method increases the matching speed. For the image feature matching system, it means that the method can afford the identification result in a shorter time than the non-serialized one. In WTS, it can be utilized to improve identification efficiency.

VI. CONCLUSION

Wood product identification is an important technology in WTS. Traditional image-based methods employ the Gaussian blur method to get the key features of the image, but the texture of the wood product often is slim, which is hard to be detected using the transitional feature detection method. In this study, we utilized a nonlinear method AKAZE to detect the texture feature. This method is based on the heat conduction theory, which could provide better performance to detect the features of the textures. A sub-area of the image method and a serialized method were also used to speed up the matching time.

The wood texture is an innate structure that has anisotropy. The experiments demonstrated that the AKAZE based method has the ability to extract the unique texture feature of the wood product. This feature can be used to distinguish the individual product. According to the experimental data, it was revealed that this method yields better accuracy and robustness than SIFT, ORB, and SURF methods, such that the $F1$, accuracy and recall of the AKAZE reached 0.96, 0.98, and 0.96, respectively. We proposed a new sub-image filter and serialization methods that were utilized to speed up the matching time of the identification. The findings clearly showed that these two methods can reduce the matching time up to 1/3 of original image matching.

All in all, this method uses the innate biometric as the identifier with no attached labels such as QR code or RFID, and it is unique and secure. It is a feasible way to use this improved method to identify the individual wood product. This study also can be taken into account to distinguish other real things which contain unique texture on the surface.

REFERENCES

[1] P. Baas, "Atlas of macroscopic wood identification: With a special focus on timbers used in Europe and CITES-listed species," *IAWA J.*, vol. 41, no. 2, pp. 259–260, May 2020.

[2] V. Sharma, J. Yadav, R. Kumar, D. Tesarova, A. Ekielski, and P. K. Mishra, "On the rapid and non-destructive approach for wood identification using ATR-FTIR spectroscopy and chemometric methods," *Vibrational Spectrosc.*, vol. 110, Sep. 2020, Art. no. 103097.

[3] J. Godbout, C. Bomal, K. Farr, M. Williamson, and N. Isabel, "Genomic tools for traceability: Opportunities, challenges and perspectives for the Canadian forestry sector," *Forestry Chronicle*, vol. 94, no. 01, pp. 75–87, Jan. 2018.

[4] S. Figorilli, F. Antonucci, C. Costa, F. Pallottino, L. Raso, M. Castiglione, E. Pinci, D. D. Vecchio, G. Colle, A. R. Proto, G. Sperandio, and P. Menesatti, "A blockchain implementation prototype for the electronic open source traceability of wood along the whole supply chain," *Sensors*, vol. 18, no. 9, pp. 1–12, 2018.

[5] S. Kannangara, S. Karunarathne, L. Ranaweera, K. Ananda, D. Ranathunga, H. Jayarathne, C. Weebadde, and S. Sooriyapathirana, "Assessment of the applicability of wood anatomy and DNA barcoding to detect the timber adulterations in Sri Lanka," *Sci. Rep.*, vol. 10, no. 1, p. 4352, Dec. 2020.

[6] T. He, L. Jiao, M. Yu, J. Guo, X. Jiang, and Y. Yin, "DNA barcoding authentication for the wood of eight endangered dalbergia timber species using machine learning approaches," *Holzforschung*, vol. 73, no. 3, pp. 277–285, Mar. 2019.

[7] E. E. Dormontt, M. Boner, B. Braun, G. Breulmann, B. Degen, E. Espinoza, S. Gardner, P. Guillery, J. C. Hermanson, G. Koch, S. L. Lee, M. Kanashiro, A. Rimbawanto, D. Thomas, A. C. Wiedenhoeft, Y. Yin, J. Zahnen, and A. J. Lowe, "Forensic timber identification: It's time to integrate disciplines to combat illegal logging," *Biol. Conservation*, vol. 191, pp. 790–798, Nov. 2015.

[8] A. J. Lowe and H. B. Cross, "The application of DNA methods to timber tracking and origin verification," *IAWA J.*, vol. 32, no. 2, pp. 251–262, 2011.
[9] L. H. Tnah, S. L. Lee, K. K. S. Ng, S. Bhassu, and R. Y. Othman, "DNA extraction from dry wood of neobalanocarpus heimii (Dipterocarpaceae) for forensic DNA profiling and timber tracking," *Wood Sci. Technol.*, vol. 46, no. 5, pp. 813–825, Sep. 2012.
[10] L. Zhao and J. Wang, "The method of identifying the species of coniferous wood based on GLCM," *J. Coastal Res.*, vol. 103, no. sp1, p. 570, Jun. 2020.
[11] R. Schraml, K. Entacher, A. Petutschnigg, T. Young, and A. Uhl, "Matching score models for hyperspectral range analysis to improve wood log traceability by fingerprint methods," *Mathematics*, vol. 8, no. 7, p. 1071, Jul. 2020.
[12] H. Rajagopal, A. S. M. Khairuddin, N. Mokhtar, A. Ahmad, and R. Yusof, "Application of image quality assessment module to motion-blurred wood images for wood species identification system," *Wood Sci. Technol.*, vol. 53, no. 4, pp. 967–981, Jul. 2019.
[13] S.-W. Hwang, K. Kobayashi, S. Zhai, and J. Sugiyama, "Automated identification of Lauraceae by scale-invariant feature transform," *J. Wood Sci.*, vol. 64, no. 2, pp. 69–77, Apr. 2018.
[14] T. Pahlberg, O. Hagman, and M. Thurley, "Recognition of boards using wood fingerprints based on a fusion of feature detection methods," *Comput. Electron. Agricult.*, vol. 111, pp. 164–173, Feb. 2015.
[15] R. Schraml, H. Hofbauer, A. Petutschnigg, and A. Uhl, "On rotational pre-alignment for tree log identification using methods inspired by fingerprint and iris recognition," *Mach. Vis. Appl.*, vol. 27, no. 8, pp. 1289–1298, Nov. 2016.
[16] E. Oyallon and J. Rabin, "An analysis of the SURF method," *Image Process. Line*, vol. 5, pp. 176–218, Jul. 2015.
[17] Z. Huijuan and H. Qiong, "Fast image matching based-on improved SURF algorithm," in *Proc. Int. Conf. Electron., Commun. Control (ICECC)*, Sep. 2011, pp. 1460–1463.
[18] E. Trundle, "Sift," *Prairie Schooner*, vol. 86, no. 1, pp. 85–100, 2012.
[19] L. Zhuo, Z. Geng, J. Zhang, and X. G. Li, "ORB feature based Web pornographic image recognition," *Neurocomputing*, vol. 173, pp. 511–517, Jan. 2016.
[20] C. Ma, X. Hu, J. Xiao, H. Du, and G. Zhang, "Improved ORB algorithm using three-patch method and local gray difference," *Sensors*, vol. 20, no. 4, p. 975, Feb. 2020.
[21] S. A. K. Tareen and Z. Saleem, "A comparative analysis of SIFT, SURF, KAZE, AKAZE, ORB, and BRISK," in *Proc. Int. Conf. Comput., Math. Eng. Technol. (iCoMET)*, Mar. 2018, pp. 1–10.
[22] C. Geng and X. Jiang, "Face recognition using sift features," in *Proc. 16th IEEE Int. Conf. Image Process. (ICIP)*, Nov. 2009, pp. 3313–3316.
[23] S. Matuska, R. Hudec, P. Kamencay, M. Benco, and M. Zachariasova, "Classification of wild animals based on SVM and local descriptors," in *Proc. AASRI Conf. Circuit Signal Process. (CSP)*, vol. 9, 2014, pp. 25–30. [Online]. Available: https://www.sciencedirect.com/science/article/pii/S2212671614001061, doi: 10.1016/j.aasri.2014.09.006.
[24] M. Kharbach, R. Kamal, M. A. Mansouri, I. Marmouzi, J. Viaene, Y. Cherrah, K. Alaoui, J. Vercammen, A. Bouklouze, and Y. V. Heyden, "Selected-ion flow-tube mass-spectrometry (SIFT-MS) fingerprinting versus chemical profiling for geographic traceability of moroccan argan oils," *Food Chem.*, vol. 263, pp. 8–17, Oct. 2018.
[25] P. Sermanet and Y. LeCun, "Traffic sign recognition with multi-scale convolutional networks," in *Proc. Int. Joint Conf. Neural Netw.*, Jul. 2011, pp. 2809–2813.
[26] S. Magdy, Y. Abouelseoud, and M. Mikhail, "Privacy preserving search index for image databases based on SURF and order preserving encryption," *IET Image Process.*, vol. 14, no. 5, pp. 874–881, Apr. 2020.
[27] W. He, T. Yamashita, H. Lu, and S. Lao, "SURF tracking," in *Proc. IEEE 12th Int. Conf. Comput. Vis.*, Sep. 2009, pp. 1586–1592.
[28] E. Rublee, V. Rabaud, K. Konolige, and G. Bradski, "ORB: An efficient alternative to SIFT or SURF," in *Proc. Int. Conf. Comput. Vis.*, Nov. 2011, pp. 2564–2571.
[29] S. K. Sharma and K. Jain, "Image stitching using AKAZE features," *J. Indian Soc. Remote Sens.*, vol. 48, no. 10, pp. 1389–1401, Oct. 2020.
[30] J. Simonović, J. Stevanic, D. Djikanović, L. Salmén, and K. Radotić, "Anisotropy of cell wall polymers in branches of hardwood and softwood: A polarized FTIR study," *Cellulose*, vol. 18, no. 6, pp. 1433–1440, Dec. 2011.
[31] D. Yang, S. Yoo, I. Doh, and K. Chae, "Selective blockchain system for secure and efficient D2D communication," *J. Netw. Comput. Appl.*, vol. 173, Jan. 2021, Art. no. 102817.
[32] M. Jo, K. Hu, R. Yu, L. Sun, M. Conti, and Q. Du, "Private blockchain in industrial IoT," *IEEE Netw.*, vol. 34, no. 5, pp. 76–77, Sep. 2020.
[33] D. Prashar, N. Jha, S. Jha, Y. Lee, and G. P. Joshi, "Blockchain-based traceability and visibility for agricultural products: A decentralized way of ensuring food safety in India," *Sustainability*, vol. 12, no. 8, p. 3497, Apr. 2020.
[34] A. Kaur, A. Nayyar, and P. Singh, *Cryptocurrencies and Blockchain Technology Applications, Chapter Blockchain: A Path to the Future*. Hoboken, NJ, USA: Wiley, 2020, pp. 25–42.
[35] S. Appelhanz, V.-S. Osburg, W. Toporowski, and M. Schumann, "Traceability system for capturing, processing and providing consumer-relevant information about wood products: System solution and its economic feasibility," *J. Cleaner Prod.*, vol. 110, pp. 132–148, Jan. 2016.
[36] R. Schraml, J. Charwat-Pessler, A. Petutschnigg, and A. Uhl, "Towards the applicability of biometric wood log traceability using digital log end images," *Comput. Electron. Agricult.*, vol. 119, pp. 112–122, Nov. 2015.
[37] P. F. Alcantarilla, A. Bartoli, and J. Andrew Davison, "KAZE Features," in *Computer Vision—ECCV* (Lecture Notes in Computer Science Including Subseries Lecture Notes in Artificial Intelligence and Lecture Notes in Bioinformatics). Berlin, Germany: Springer, 2012, pp. 214–227.
[38] V. V. Nabiyev, S. Yilmaz, A. Günay, G. Muzaffer, and G. Ulutaş, "Shredded banknotes reconstruction using AKAZE points," *Forensic Sci. Int.*, vol. 278, pp. 280–295, Sep. 2017.
[39] C. Meixi, Y. Yule, and Z. Yong, "KAZE feature point with modified-SIFT descriptor," in *Proc. 3rd Int. Conf. Multimedia Technol. (ICMT)*, Paris, France, 2013, pp. 1250–1258.
[40] H. Bay, A. Ess, T. Tuytelaars, and L. Van Gool, "Speeded-up robust features (SURF)," *Comput. Vis. Image Understand.*, vol. 110, no. 3, pp. 346–359, Jun. 2008.
[41] S. Zhang, X. Li, M. Zong, X. Zhu, and R. Wang, "Efficient kNN classification with different numbers of nearest neighbors," *IEEE Trans. Neural Netw. Learn. Syst.*, vol. 29, no. 5, pp. 1774–1785, May 2018.
[42] Z. Zhang, "Introduction to machine learning: K-nearest neighbors," *Ann. Transl. Med.*, vol. 4, no. 11, p. 218, 2016.
[43] L. Zhang, P. Shen, G. Zhu, W. Wei, and H. Song, "A fast robot identification and mapping algorithm based on kinect sensor," *Sensors*, vol. 15, no. 8, pp. 19937–19967, Aug. 2015.
[44] H. M. Weik, "Hamming distance," in *Computer Science and Communications Dictionary*. Boston, MA, USA: Springer, 2000, p. 706.
[45] A. M. Fischler and C. R. Bolles, "Random sample consensus: A paradigm for model fitting with applications to image analysis and automated cartography," *Commun. ACM*, vol. 24, no. 6, pp. 381–395, Jun. 1981.
[46] J. Lever, M. Krzywinski, and N. Altman, "Classification evaluation," *Nature Methods*, vol. 13, no. 8, pp. 603–604, Aug. 2016.
[47] D. M. W. Powers, "Evaluation: From precision, recall and F-measure to ROC, informedness, markedness and correlation," *J. Mach. Learn. Technol.*, vol. 2, no. 1, pp. 37–63, 2011.
[48] A. Puri and M. K. Gupta, "Comparative analysis of resampling techniques under noisy imbalanced datasets," in *Proc. Int. Conf. Issues Challenges Intell. Comput. Techn. (ICICT)*, Sep. 2019, pp. 1–5.
[49] P. G. Rédei, "Euclidean distance," in *Encyclopedia of Genetics, Genomics, Proteomics and Informatics*. Dordrecht, The Netherlands: Springer, 2008, p. 638.
[50] L. Zhang, Y. Zhang, J. Tang, K. Lu, and Q. Tian, "Binary code ranking with weighted Hamming distance," in *Proc. IEEE Conf. Comput. Vis. Pattern Recognit.*, Jun. 2013, pp. 1586–1593.

YONGKE SUN was born in Xianyang, Shanxi, China, in 1980. He received the M.S. degree from Yunnan University, in 2012. He is currently pursuing the Ph.D. degree with Southwest Forestry University. Since 2003, he has been with Southwest Forestry University, where he works as an Associate Professor. His research interests include big data, network security, and computer-aided wood identification.

GUANBEN DU received the Ph.D. degree in wood science and technology from Nanjing Forestry University, China, in 1998. He was appointed as a Full and Chair Professor with the College of Materials Science and Engineering, Southwest Forestry University, China. He was elected as a Fellow of the International Academy of Wood Science, in 2010, the Dean of the College of Materials Science and Engineering, in 2003, and the Vice President of Southwest Forestry University, in 2007. He worked as a PI for establishing the Sino-French Laboratory and the International Joint-Research Center based on ''one belt, one road'' policy. As a Director, he has been successfully building multi research platforms, such as the Yunnan Provincial Key Laboratory of Wood Adhesives and Glued Products, the Research and Development Center for Wood-Based Composites, and the Engineering Center for Wooden Engineering Materials. He is currently working as the Director of the International Joint Research Center for Bio-Materials. He has been deeply involved in the international collaboration, such as EU Project and Sino-French Collaboration Program.

YONG CAO received the Ph.D. degree in computer application technology from the University of Electronic Science and Technology of China, in 2010. Since 2011, he has been an Associate Professor with Southwest Forestry University. He is a Co-Founder of the International Engineering and Technology Institute (IETI). He is an expert in the field of computer science. His main research interests include complex networks, machine learning, bioinformatics, computer-aided wood identification, nonlinear science, and software engineering.

QIZHAO LIN was born in Sanming, Fujian, China, in 1982. He received the Ph.D. degree from Southwest Forestry University, in 2020. Since 2008, he has been with Southwest Forestry University. He is currently an Engineer in the field of computer science. The Softwood Retrieval System (http://woodlab.swfu.edu.cn) is his newest result of scientific research. His main research interests include deep learning and computer-aided wood identification.

LIHUI ZHONG was born in Lijiang, Yunnan, China, in 1984. She received the M.S. degree in electrical engineering from Zhengzhou University, in 2010. She was with Southwest Forestry University. She is currently a Lecturer. Her research interests include computer-aided wood identification and signal processing.

JIAN QIU was born in Kunming, Yunnan, China, in 1965. He received the Ph.D. degree from Northeast Forestry University, in 2004. He is currently pursuing the Ph.D. degree with Southwest Forestry University. He is currently a second-class Professor in teaching and research of wood science and technology with Southwest Forestry University. He is also the Executive Director of the Wood Science Branch of China Forestry Association, the Executive Director of the IAWA China Branch of International Association of Wood Anatomists, the National Award Review Expert, a member of the Expert Review Group of NSFC, the Deputy Director of the Academic Committee of Southwest Forestry University, and a member of the National Wood Standards Committee.